ARTICLES

Dual Ensemble Monte Carlo Simulation of Pervaporation of an Ethanol/Water Binary Mixture in Silicalite Membrane Based on a Lennard-Jones Interaction Model

Hiromitsu Takaba,* Akio Koyama, and Shin-ichi Nakao

Department of Chemical System Engineering, School of Engineering, The University of Tokyo, 7-3-1 Hongo, Bunkyo-ku, Tokyo 113-8656, Japan

Received: December 13, 1999; In Final Form: March 22, 2000

A recently developed dual ensemble Monte Carlo (DE-MC) simulation has been applied to the study of pervaporation of a Lennard-Jones (LJ) fluid mixture, modeled for an ethanol and water mixture, occurring in MFI-type silicalite membrane. From the simulation results for the binary system, it is indicated that ethanol LJ molecules can readily enter the membrane pore, whereas no water LJ molecules penetrate into the pore, resulting in the formation of an adsorbed phase with the silanol groups on the external surface. The molecular density profile obtained for the binary system clearly reveals the adsorption site of ethanol, and it was found that the amount of adsorbed ethanol in the membrane decreases linearly from the feed side to the vacuum side. The total extent of ethanol adsorption in the membrane pore from the binary mixture is smaller than that from the pure liquid component when the ethanol activity is the same. These observed behaviors are in qualitative agreement with experimental observations.

1. Introduction

Because pervaporation is one of the most energy-efficient separation technologies, a great deal of research relating to its industrial application has been reported.[1−14] Usually this technique is employed to enhance a valuable or small amount of a component in an organic binary mixture or in aqueous solution. Recently, in addition to research using organic membranes, some studies using zeolite membranes have been reported.[3−15] The selectivity of zeolite membranes is characterized by the hydrophobicity or hydrophilicity of the zeolite, in addition to its shape selectivity, which depends on the type of zeolite and the alumina content in the zeolite framework. Siliceous MFI-type zeolite (silicalite) shows high hydrophobicity, whereas high-alumina-content zeolites, e.g., A-type, Y-type, and ZSM-5 zeolites, show high hydrophilicity. Sano et al.[3,6,7] synthesized a silicalite membrane on a stainless steel support and found a high selectivity for C1−C4 alcohols in aqueous solution. Kita et al.[5,9] reported a highly water-selective A-type zeolite membrane. Therefore, for designing the appropriate zeolite membrane for a pervaporation process, it is important to determine the surface properties and shape selectivity of the zeolite membrane.

In theoretical studies, the sorption−diffusion model generally describes the transport mechanism of pervaporation. According to the model, the solubility and diffusivity of solvent to membrane may enable a prediction of the performance of a membrane.[16] However, reported zeolite membranes usually have a grain boundary, which is considered to contribute significantly to the selectivity, and therefore, the mechanism of pervaporation using a zeolite membrane is rather complicated. Wegner et al.[12] investigated the pervaporation of xylene isomers on a ZSM-5 membrane and tried to explain the experimental results supposing that the presence of the microporous nonzeolitic pores played an important role in the selectivity. Nomura et al.[15] synthesized the silicalite membrane and tried to plug the cracks in the silica using the chemical vapor deposition technique. Modification of the membrane decreased the flux of solvent, while the selectivity increased. Those studies imply that the observed selectivity of zeolite membrane is significantly influenced by the structure of the membrane. Therefore, although a great deal of work related to the pervaporation process has been published, detailed information on an atomistic level is still needed for a better understanding of the process.

Recently, computer simulation studies of the adsorption and diffusion of molecules inside zeolites, based on accurate intermolecular potentials, have been published.[17−22] However, to our knowledge, the simulation of pervaporation in inorganic membranes has not been reported. This is probably because of the large computational time required. In this study, a recently developed dual ensemble Monte Carlo technique,[23,24] co-developed by one of the authors, is used for the simulation. This technique has been developed on the basis of the grand canonical ensemble Monte Carlo method intended to treat a nonequilibrium system in which a chemical potential gradient exists. The DE-MC method has an advantage in CPU time compared with alternative approaches for simulating a nonequilibrium condition, because the DE-MC method treats the movement of molecules in a stochastic manner. Therefore, a steady state of permeation is easily achieved with minimal CPU time.

Recently, we noticed that a concept similar to DE-MC has

* Author to whom correspondence should be addressed. Telephone: +81-3-5841-8839. Fax: +81-5841-7279. E-mail: takaba@nakao1.t.u-tokyo.ac.jp.

10.1021/jp994384v CCC: $19.00
Published on Web 06/16/2000

been presented by Papadopoulou et al.[25] Their proposed concept, called a *local* GCMC method, has been applied to one-dimensional lattice gas and hard-sphere systems, as well as to a three-dimensional bulk Lennard-Jones (LJ) system, and carefully compared with the results of grand canonical ensemble molecular dynamics (GCMD). The DE-MC method could be considered as the extension of this method to simulate the nonequilibrium condition suitable for calculations on a membrane system.

In the present study, we applied the DE-MC technique to investigate the pervaporation of a LJ mixture modeled for an ethanol/water binary mixture occurring in MFI-type silicalite membrane and tried to describe the process at a microscopic level. As a first attempt for the simulation of pervaporation in inorganic membranes, a spherical LJ-type model was used for representing both ethanol and water molecules. The main objectives of our study were, therefore, the following: to qualitatively describe the separation performance of ethanol from an aqueous solution on a zeolite membrane with a perfect crystal and to investigate the molecular distribution in the membrane pore when the pervaporation occurs. An atomistic understanding of the pervaporation process will be helpful for both developing membrane materials and exploring novel applications.

2. Methodology and Model

2.1. DE-MC Simulation. The DE-MC method employs a grand canonical (μVT) ensemble MC technique in combination with a canonical (NVT) ensemble MC technique.[23,24] The chemical potential gradient is introduced in the unit cell by dividing the unit cell into several parts and maintaining each part at a different chemical potential. Figure 1 shows the geometry of the unit cell used in this study. The unit cell is separated into four regions, namely *A*, *B*, *C*, and *D*. Chemical potentials in two distinct regions correspond to two different reservoir regions, which are indicated in Figure 1 as region *B* with a high chemical potential and region *D* with a low chemical potential. In region *C*, only the displacement of particles is permitted. The displacement of particles in region *C* is simulated using the canonical ensemble MC method and is expected to distribute according to the chemical potential gradient between the two reservoirs. If the membrane model is located in region *C*, we can simulate the flow of particles through the membrane between these two reservoirs. Region *A* is fixed to prevent the periodic displacement of particles. Every 50 000 steps, the molecules in region *A* are exchanged using μVT ensemble MC techniques to satisfy the solvent density at a specified temperature, and their positions are kept fixed for the next 50 000 steps. This exchange of molecules is performed so that the influence of the uniform molecular layer in region *A* on the molecular distribution in region *B* is small. In the following calculations, the chemical potential in region *D* is maintained at zero, thus assuming a vacuum condition.

The particles are inserted and destroyed in regions *B* and *C* by the normal GCMC prescription in order to maintain the chemical potential in both phases at the desired level. We used the Metropolis algorithm in which configurations are generated by three kinds of particle movement: creation, removal, and displacement.[26] Creation is accepted with a probability given by

$$p = \min\left\{1, \left[\left(\frac{fV}{kT}\right)/(N+1)\right] \exp(-\Delta E/kT)\right\} \qquad (1)$$

where ΔE is the change in the potential ($\Delta E = \Delta E_{new} - \Delta E_{old}$), k is the Boltzmann constant, T is the temperature, and N is the number of molecules present before the attempted creation. The volume V refers to the volume in the distinct region. The fugacity, f, is estimated by the Lee-Kesler equation,[27] as indicated in the following equation

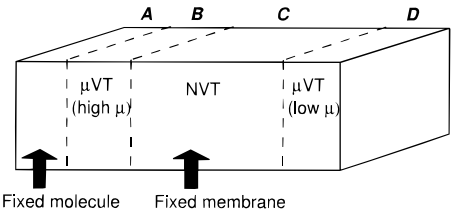

Figure 1. Schematic representation of the unit cell used in the DE-MC simulations.

$$\ln \frac{f}{P} = \frac{S - S^0}{R} - \frac{H - H^0}{RT} \qquad (2)$$

where S is the entropy and H is the enthalpy. Superscript 0 means the reference. P is the pressure of a specific species. The relationship of S and H to P is summarized as a table in ref 27.

Removal is accepted with probability

$$p = \min\left\{1, \left[N/\left(\frac{fV}{kT}\right)\right] \exp(-\Delta E/kT)\right\} \qquad (3)$$

Displacement in the region is accepted with a probability given by

$$p = \min\{1, \exp(-\Delta E/kT)\} \qquad (4)$$

For particles in region *C*, only the displacement is attempted as in the *NVT* ensemble, because the number of particles is held constant during the displacement.

The magnitude of displacement (dmax) is 0.4 Å. Papadopoulou et al.[25] mentioned, in their report relating to the *local* GCMC method, that dmax is not related to the possibility of the acceptance of the displacement procedure as in the conventional MC technique. They further noted that taking a large dmax value is effective for a fast approach to equilibrium, e.g., dmax = 1.5σ (where σ is the Langmuir parameter of the particle). We also confirmed that a large value of dmax gives a rapid achievement of equilibrium; however, sometimes it fails to produce a realistic molecular distribution in the unit cell. At the least, the maximum dmax value might be less than the minimum distance between adsorption sites in the zeolite framework. We simulated an argon gas distribution in a silicalite membrane under a chemical potential gradient using the GCMD method and compared the GCMD result with the DE-MC result for the same system. It was found that a small dmax value in the DE-MC calculation always gives the molecular distribution equivalent to that obtained by the GCMD technique. Hence, we used a small dmax value of 0.4 Å for all calculations.

The cutoff length for interaction was fixed at 10 Å. A three-dimensional periodic boundary condition was applied to the unit cell. The size of the unit cell used in this study is 20.022 Å × 120.000 Å × 26.766 Å, except for the vapor phase simulation. The dimensions of each region along the flow direction are 0−16.8 Å for region *A*, 16.8−28.8 Å for region *B*, 28.8−66.0 Å for region *C*, and 66.0−120.0 Å for region *D*. All simulations were performed at 303 K. The total number of simulation steps was 10 000 000, which was enough to reach equilibrium of total energy and loading of the system, and we monitored the last 2 000 000 steps for the statistical analysis.

TABLE 1: Potential Parameters Used in This Study[a]

atom	e/k (K)	σ (Å)
Si−Si	20.2126	4.5498
O−O	115.212	3.21
H−H	13.5	2.75
EtOH	485.101	4.93
H_2O	809.109	3.3
EtOH−Si	60.635	4.7399
EtOH−O	112.28	4.14
H_2O−Si	50.5295	3.9249
H_2O−O	42.4448	3.7
EtOH−H_2O	313.244	4.115

[a] The 12−6 Lennard Jones potential is assumed to be the function $E_{ij} = 4e_{ij}[(\sigma_{ij}/r_{ij})^{12} - (\sigma_{ij}/r_{ij})^6]$. The parameters for the Si−Si, O−O, and H−H atom interactions are derived from the CVFF force-field set. Detailed information was presented in ref 32. The parameters for Si−Si, O−O, and H−H are not used in the DE-MC simulations

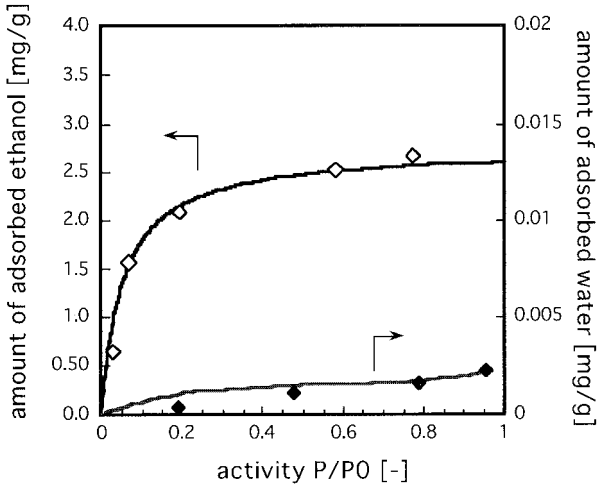

Figure 2. Calculated adsorption isotherms of ethanol and water using an optimized interatomic potential. Symbols represent the DE-MC result, while experimental data are indicated by solid lines. Temperature is 303 K. P_0 means vapor pressure, 10.47 kPa for EtOH and 4.24 kPa for H_2O.

We used the RYUGA code to obtain the 3-dimensional pictures.[28]

2.2. Potential. The solvent−solvent, as well as the solvent−framework, interaction is described by a LJ (12-6) type of potential. The parameters of the interatomic potential used in our study are listed in Table 1. We treat both CH_3CH_2OH (EtOH) and H_2O (water) molecules as LJ fluids (single-sphere model) in order to perform the simulation for a reasonably long time and large system. This approximation neglects the orientation of the molecules and the dipole moment but yields standard results with which more complicated and realistic systems can be compared. We modified the parameters for the solvents (EtOH and H_2O) reported in ref 27 so that they reproduce each solvent density at 303 K. The LJ parameters of the H, Si, and O atoms in the zeolite framework are taken from the CVFF force-field set, which was optimized for zeolite systems.[29,30] The interatomic potential between EtOH and H_2O in the LJ terms is estimated by adapting the Lorentz−Berthelot mixing rule,[26] while the interatomic potential between solvents and atoms in silicalite in the LJ terms is determined to reproduce the experimental isotherms, based on the CVFF force field.

Figure 2 presents a comparison of the calculated result of isotherms for EtOH and H_2O in silicalite with experimental data. The temperature was 303 K. The isotherms were simulated by conventional grand canonical ensemble MC techniques using two silicalite unit cells. One million MC steps were performed, and the last 500 000 steps were used to estimate the amount of adsorption. The cutoff length was 10 Å. As shown in this figure, the calculated results agree well with experiment for both H_2O and EtOH and reproduce well the hydrophobic nature of silicalite. In the following calculations, we used this potential parameter set.

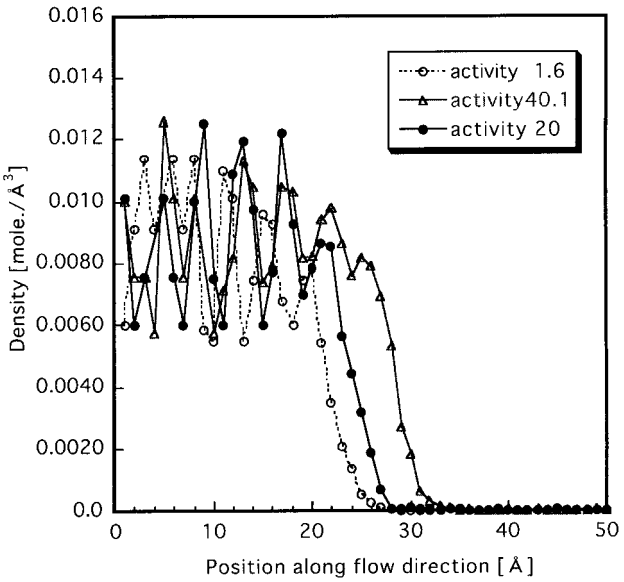

Figure 3. Calculated density profiles of ethanol in the unit cell without the membrane. Three results for ethanol activities of 1.6, 20.0, and 40.1 are indicated.

2.3. Membrane Model. The MFI-type silicalite crystal structure used in this study is presented in the *Pnma* space group (orthorhombic), with lattice parameters $a = 20.022$ Å, $b = 19.899$ Å, and $c = 13.383$ Å.[31] The silicalite structure has two types of channel: a straight channel running parallel to the y direction and zigzag channels running along the x direction. The DE-MC unit cell, consisting of silicalite unit cells superimposed by $1 \times 1.5 \times 2$, resulted in the inclusion of 288 Si and 592 O atoms. The membrane has a (010) external surface. Hydrogen atoms were added to unsaturated surface oxygen atoms, which led to the formation of surface silanol groups. The position of all atoms in the membrane was optimized to relax the structure using molecular dynamics techniques at 303 K. The detailed methodology for the construction of the membrane surface and the interatomic potentials used for the MD calculation have been described in our previous work.[32]

3. Results and Discussion

3.1. Vapor Interface of Ethanol Liquid. First, a DE-MC calculation was performed to simulate the vapor−liquid phase of ethanol at various degrees of ethanol activity, using the MC cell not containing the membrane model. The boundaries of each cell region along the flow direction are 0−10 Å for region *A*, 10−20 Å for region *B*, 20−80 Å for region *C*, and 80−100 Å for region *D*. Figure 3 shows the calculated density profile of ethanol in the unit cell. The density profiles in regions *A* and *B* are almost flat and constant for the three systems with different activities, although there seems to be some scatter. This indicates that, in regions *A* and *B* ethanol is a liquid and that the procedure of creation and removal of molecules by the DE-MC method worked as expected. In region *C*, the density profile decreases rapidly and becomes zero. This result indicates that a vapor−liquid phase exists in this region. The transition point of the

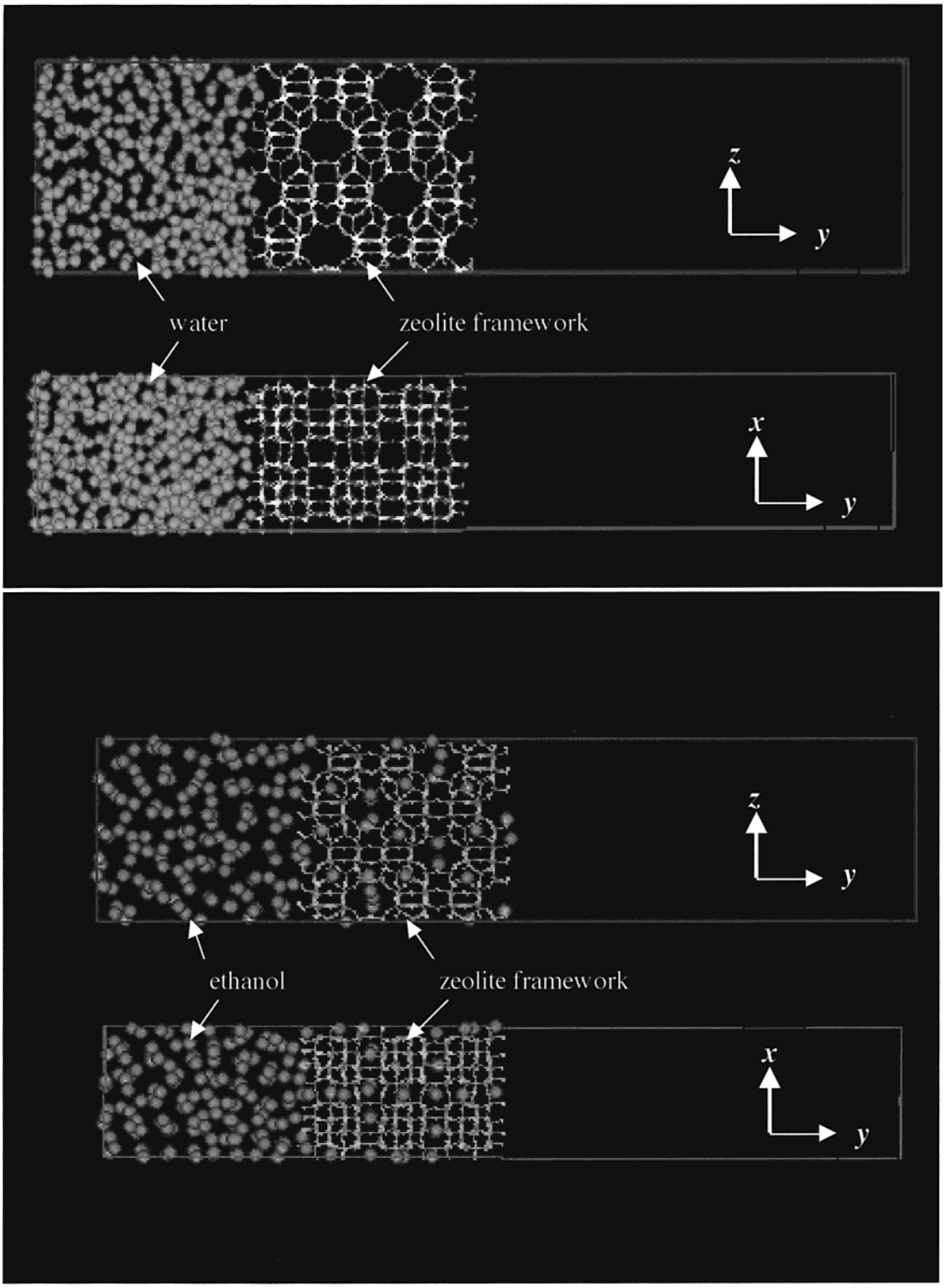

Figure 4. Computer graphics pictures of the DE-MC results. These pictures represent the equilibrium molecular distributions in the unit cell (a) for water and (b) for ethanol. Solvent molecules are presented as a sphere model, while the silicalite membrane is presented as a framework model. Only ethanol molecules entered the silicalite pore.

vapor−liquid phase moves to the right with increasing activity of ethanol. The transition point of the vapor−liquid phase is expected to move farther from the controlled region (region *A*) with increasing activity, assuming that the chemical potential gradually decreases between the two controlled reservoirs. From this result, it is suggested that a reliable chemical potential gradient can be reproduced by the DE-MC method.

3.2. Pure Liquid. The micropore of silicalite is hydrophobic. However, the membrane surface facing the gas phase is expected to show a slight hydrophilic property, because the external surface of silicalite is covered with silanol groups. Although in a DE-MC calculation a particle moves according to a stochastic method, the DE-MC method can simulate the molecular trajectory from the feed side to the vacuum side through the external surface to simulate the effect of the external surface on the permeation. Figure 4 shows a snapshot of the DE-MC

TABLE 2: MC Parameters in Equations 1 and 3 Used for Calculations[a]

EtOH activity	EtOH mole fraction	*z* (ethanol)	*z* (water)
	Single Component		
0.15	1.0	0.5432	–
0.41	1.0	1.252	–
0.62	1.0	3.715	–
1.0	1.0	7.017	–
9.68	1.0	14.124	–
23.89 (H_2O)	–	–	0.447
	Binary Mixture		
0.15	0.009	0.01425	0.4608
0.4	0.09	0.1164	0.4565
0.6	0.5	1.862	0.4512

[a] $z = f/KT \times 10^{-30}$.

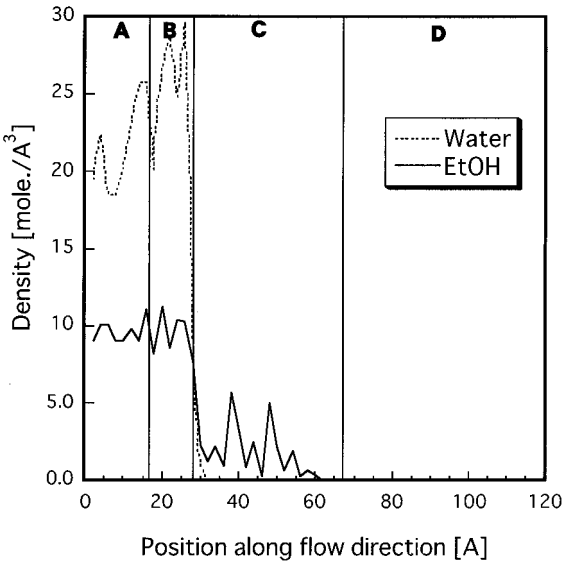

Figure 5. Calculated density profiles of pure solvent in the unit cell with a silicalite membrane. Both results for ethanol and water are presented.

result for pure liquid systems after they have reached equilibrium. The pressure of the systems was set at atmospheric pressure (101.3 kPa); the corresponding fugacity is listed in Table 2. From this picture, we find that no water molecules penetrate into the pore, whereas ethanol molecules exist in the pore and are distributed throughout the pore, including the zigzag channels, the straight channels, and the intersection sites. The results obtained demonstrate the high hydrophobicity of silicalite.

Figure 5 shows the density profile for the pure liquids. The density of water in region *B* increases on approaching the membrane surface, which means that an adsorbed phase was formed on the external surface because of the interaction with the silanol groups. In addition to the hydrophobic property of the zeolite pore, adsorption of water at the entrance of the membrane pore seems to prevent the penetration of water. On the other hand, the density of ethanol near the surface remains almost the same as that in region *A*. This means that significant ethanol adsorption on the surface does not occur. In region *C*, a tall distinct peak in the density profile of ethanol is observed. Two distinct peaks in region *C* correspond to adsorption at a zigzag channel and an intersection site, whereas the lower three peaks correspond to adsorption at the middle of the straight channel between intersections.

It is noted that the density decreases gradually from the feed side to the vacuum side. Recently, gas permeation in silicalite membranes under steady-state conditions was investigated by the GCMD technique.[33] It was reported that the molecular density of gas in the zeolite pore along the flow direction decreases linearly from the feed side to the permeate side, corresponding to the decrease in chemical potential. This means that the gradient in the molecular density is also found in the pervaporation of silicalite as well as in gas permeation.

3.3. Binary Mixture. A DE-MC simulation was performed for the system including two solvents on a silicalite membrane. We kept the ratio of ethanol/water mixture in region *A* constant during the simulation. The fugacities of the binary mixtures were estimated using eq 2, and they are listed in Table 2. Figure 6 presents a steady-state snapshot of the DE-MC result, when the ethanol concentration on the feed side was kept at a mole fraction of 0.09. Only ethanol molecules penetrate into the pore, whereas no water penetrates. This selective penetration behavior is similar to the results for the simulation of pure components. Indeed, the penetration behavior was not significantly influenced by interaction between water and ethanol molecules, even in the binary system. In addition, in other calculations with different mixture ratios, no water penetrates into the membrane pore. This implies that the silicalite membrane having a perfect structure modeled in this simulation shows a high selectivity for ethanol. In experimental studies, it is well-known that silicalite membranes show a high selectivity for ethanol in aqueous solution. For example, Sano et al.[3] reported that the separation factor of ethanol is higher than 60 for a 0.02 mole fraction at 303 K. Considering that the experimental membrane contains a grain boundary region, such experimental data support our simulation results.

Figure 7 shows the density profile of ethanol in a binary mixture along the flow direction. Two simulation results for ethanol concentrations of 0.09 and 0.009 mole fraction are presented. Only the density of the *C* region is indicated. The density of water is omitted because it is almost zero. Three distinct peaks correspond to adsorption at a zigzag channel and intersection, and the other lower three peaks correspond to adsorption at the middle of a straight channel between intersections. Ethanol density at the middle of a straight channel was found only when the mole fraction of ethanol was 0.09. The adsorption of ethanol occurred throughout all of the pore space, although adsorption at the middle of the straight channel was observed only when the ethanol activity was rather high.

The density shown in Figure 7 clearly decreases from the feed side to the vacuum side. Pervaporation is accompanied by a phase change of solvent from liquid to gas. If a phase change occurs inside the membrane, the change of the density in the membrane region will be heterogeneous. Because the calculated density in the membrane region changes homogeneously, the phase transition occurs at around the membrane surface in these simulations. Moreover, the density of ethanol in the membrane pore is lower than that in regions *A* and *B*, which means that the ethanol in the membrane is not liquid.

Figure 8 shows a comparison of the amount of adsorption of ethanol in the membrane for pure and binary systems as a function of ethanol activity in region *B*. The amount of adsorption in binary mixture systems is much smaller than that in pure systems. The adsorbed phase of water on the external surface might make the penetration of ethanol difficult. Nomura et al.[4] measured ethanol/water adsorption on a silicalite membrane using gravimetric and adsorption−desorption methods. It was reported that the adsorption of ethanol in binary aqueous solutions becomes small compared with that of the pure system, which is consistent with our DE-MC result. Moreover, our DE-

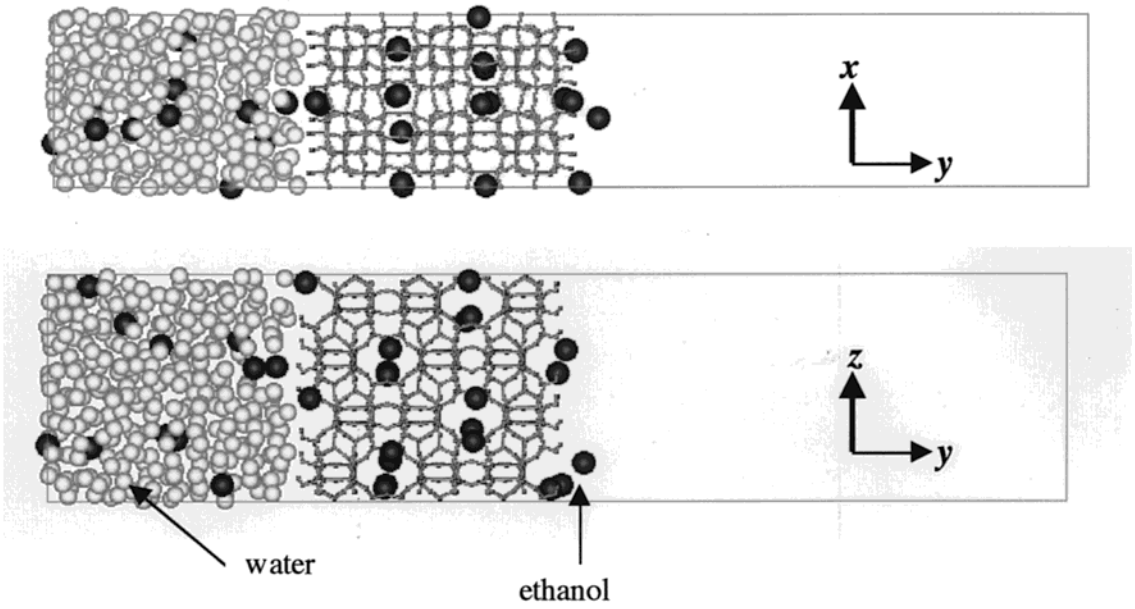

Figure 6. Computer graphics pictures of the DE-MC results for an ethanol/water mixture with an ethanol concentration of 0.09 mole fraction. Larger spheres represent ethanol, while smaller spheres represent water molecules. Only ethanol molecules entered the silicalite pore.

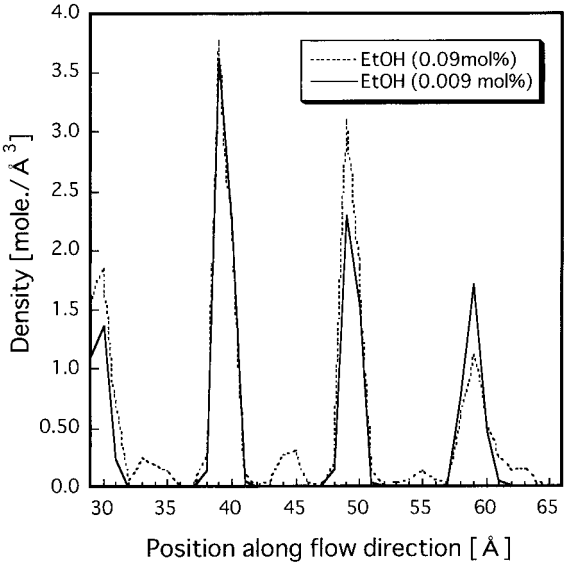

Figure 7. Calculated density profiles of ethanol in the unit cell for an ethanol/water mixture. Only the results in region *C* are indicated. The solid line is the result for an ethanol concentration of 0.009 mole fraction, while the broken line is the result for a 0.09 mole fraction.

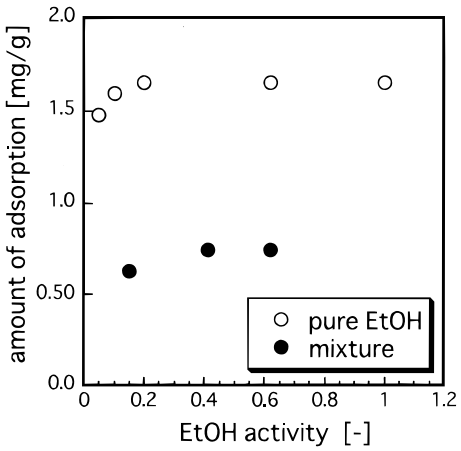

Figure 8. Amount of adsorption of ethanol in silicalite membrane as a function of ethanol activity.

MC result indicates that the ethanol adsorption does not change in a range of ethanol activity larger than 0.2; therefore, we can expect the permeability of ethanol to remain almost constant in this range, if we assume a solution−diffusion mechanism for this system.

4. Conclusion

We have successfully employed a dual ensemble Monte Carlo (DE-MC) simulation to investigate the molecular density profile in the silicalite membrane at various degrees of concentration of a LJ mixture modeled for ethanol in aqueous solution. The DE-MC calculations were performed with a LJ interatomic potential that is confirmed to be able to reproduce the experimental adsorption isotherms of water and ethanol as single components on silicalite. The simulation results indicate that ethanol molecules can readily penetrate into the membrane pore, whereas no water molecules penetrate. For both pure and binary systems, similar penetration behaviors were observed.

The obtained molecular density profile for binary systems revealed that the adsorption at a straight channel pore was observed only at high ethanol concentration. The ethanol density in the membrane decreases linearly from the feed side to the vacuum side. This result suggests that a liquid−gas phase transition occurred at the entrance of the membrane pore. The total amount of adsorption of ethanol in the pores for binary systems was smaller than that for the pure component system when the ethanol activity was the same.

In this study, the silicalite membrane was assumed to consist of a perfect crystal. As mentioned in the Introduction, an actual zeolite membrane has a polycrystalline microstructure. The qualitative agreement of our simulation results with experimental observation implies that the pervaporation through the intercrystalline region is similar to that through the zeolitic pore. However, for a full understanding of the pervaporation occurring

in this system, a study of the influence of the intercrystalline region on the permeation, as well as a study using a more accurate interaction model, will be required. Although it is still difficult to treat the unique structure of zeolites because of restrictions on computational power, a simplified model for intercrystalline region that extracts the unique structure of zeolite membrane can be studied. Now, we are attempting to study such system with a more accurate interaction model, and we will provide the results in the near future.

References and Notes

(1) Brun, J.-P.; Larchet, C.; Bulvestre, G.; Auclair, B. *J. Membr. Sci*. **1985**, *25*, 55−100.
(2) Blume, I.; Wijmans, J. G.; Baker, R. W. *J. Membr. Sci*. **1990**, *49*, 253−286.
(3) Sano, T.; Yanagishita, H.; Kiyozumi, Y.; Mizukami, F.; Haraya, K. *J. Membr. Sci*. **1994**, *95*, 221.
(4) Nomura, M.; Yamaguchi, T.; Nakao, S. *J. Membr. Sci*. **1998**, *144*, 161−171.
(5) Kita, H.; Horii, K.; Ohtoshi, Y.; Tanaka, K.; Okamoto, K. *J. Mater. Sci. Lett*. **1995**, *14*, 206.
(6) Sano, T.; Hasegawa, M.; Ejiri, S.; Kawakami, Y.; Yanagishita, H. *Microporous Mater*. **1995**, *5*, 179.
(7) Sano, T.; Ejiri, S.; Yamada, K.; Kawakami, Y.; Yanagishita, H. *J. Membr. Sci*. **1997**, *123*, 225−233.
(8) Kita, H.; Inoue, T.; Asamura, H.; Tanaka, K.; Okamoto, K. *Chem. Commun.* **1997**, *1*, 45−46.
(9) Kondo, M.; Komori, M.; Kita, H.; Okamoto, K. *J. Membr. Sci*. **1997**, *133*, 133−141.
(10) Smetana, J. F.; Falconer, J. L.; Noble, R. D. *J. Membr. Sci*. **1996**, *114*, 127−130.
(11) Liu, Q.; Noble, R. D.; Falconer, J. L.; Funke, H. H. *J. Membr. Sci*. **1996**, *117*, 163−174.
(12) Wegner, K.; Dong, J. H.; Lin, Y. S. *J. Membr. Sci*. **1999**, *158*, 17−27.
(13) Jafar, J. J.; Budd, P. M. *Microporous Mater*. **1997**, *12*, 305−311.
(14) Nishiyama, N.; Matsufuji, T.; Ueyama, K.; Matsukata, M. *Microporous Mater*. **1997**, *12*, 293−303.
(15) Nomura, M.; Yamaguchi, T.; Nakao, S. *Ind. Eng. Chem. Res*. **1997**, *36*, 4217−4223.
(16) Kataoka, T.; Tsuru, S.; Nakao, S.; Kimura. S. *J. Chem. Eng. Jpn*. **1991**, *24*, 326.
(17) Smit, B. *J. Phys. Chem.* **1995**, *99*, 5597−5603.
(18) June, R. L.; Bell, A. T.; Theodorou, D. N. *J. Phys. Chem*. **1990**, *94*, 1508−1516.
(19) Smit, B.; Daniel, L.; Loyens, J. C.; Verbist, G. L. M. M. *Faraday Discuss.* **1997**, *106*, 93−104.
(20) June, R. L.; Bell, A. T.; Theodorou, D. N. *J. Phys. Chem*. **1990**, *94*, 8232.
(21) Catlow, C. R. A.; Freeman, C. M.; Vessal, B.; Tomlinson, S. M.; Leslie, M. *J. Chem. Soc., Faraday Trans*. **1991**, *87*, 1947−1950.
(22) Hufton, J. R. *J. Phys. Chem.* **1991**, *95*, 8836−8839.
(23) Kobayashi, Y.; Kamala, C. R.; Ayappa, G.; Mizukami, K.; Oumi, Y.; Takaba, H.; Kubo, M.; Teraishi, K.; Yashonath, S.; Miyamoto, A. Proceedings of the Fifth International Conference on Inorganic Membranes, Nagoya, June 22−26, 1998; pp 648−651.
(24) Kobayashi, Y.; Mizukami, K.; Oumi, Y.; Takaba, H.; Kubo, M.; Teraishi, K.; Miyamoto, A. *Mol. Sim.*, in press.
(25) Papadopoulou, A.; Becker, E. D.; Mark, L.; van Swol, F. *J. Chem. Phys*. **1993**, *98*, 4897−4908.
(26) Allen, M. P.; Tildesley, D. J. *Computer Simulation of Liquids*; Oxford University Press: Oxford, U.K., 1987.
(27) Reid, R. C.; Prausnitz, J. M.; Poling, B. E. *The Properties of Gases & Liquids*, 4th ed.; McGraw-Hill: New York, 1988; pp 733−734.
(28) Miura, R.; Yamano, H.; Yamauchi, Y.; Kubo, M.; Miyamoto, A. *Catal. Today* **1995**, *23*, 409−416.
(29) Hill, J.-R.; Sauer, J. *J. Phys. Chem*. **1994**, *98*, 1238−1244.
(30) Hagler, A. T.; Lifson, S.; Dauber, P. *J. Am. Chem. Soc*. **1979**, *101*, 5122.
(31) Olson, D. H.; Kokotailo, G. T.; Lawton, S. L.; Meier, W. M. *J. Chem. Phys.* **1989**, *85*, 2238.
(32) Takaba, H.; Koshita, R.; Mizukami, K.; Oumi, Y.; Ito, N.; Kubo, M.; Fahmi, A.; Miyamoto, A. *J. Membr. Sci.* **1997**, *134*, 127−139.
(33) Pohl, P. I.; Heffelfinger, G. S.; Smith, D. M. *Mol. Phys.* **1996**, *89*, 1725−1731.